


# Ozone-UV-catalysis based advanced oxidation process for wastewater treatment

Martynas Tichonovas<sup>1</sup>  · Edvinas Krugly<sup>1</sup> · Dalia Jankunaite<sup>1</sup> · Viktoras Racys<sup>1</sup> · Dainius Martuzevicius<sup>1</sup>

Received: 6 March 2017 / Accepted: 29 May 2017 / Published online: 8 June 2017  
© Springer-Verlag Berlin Heidelberg 2017

**Abstract** A bench-scale advanced oxidation (AO) reactor was investigated for the degradation of six pollutants (2-naphthol, phenol, oxalic acid, phthalate, methylene blue, and D-glucose) in a model wastewater at with the aim to test opportunities for the further upscale to industrial applications. Six experimental conditions were designed to completely examine the experimental reactor, including photolysis, photocatalysis, ozonation, photolytic ozonation, catalytic ozonation, and photocatalytic ozonation. The stationary catalyst construction was made from commercially available TiO<sub>2</sub> nanopowder by mounting it on a glass support and subsequently characterized for morphology (X-ray diffraction analysis and scanning electron microscopy) as well as durability. The ozone was generated in a dielectrical barrier discharge reactor using air as a source of oxygen. The degradation efficiency was estimated by the decrease in total organic carbon (TOC) concentration as well as toxicity using *Daphnia magna*, and degradation by-products by ultra-performance liquid chromatography–mass spectrometry. The photocatalytic ozonation was the most effective for the treatment of all model wastewater. The photocatalytic ozonation was most effective against ozonation and photolytic ozonation at tested pH values. A complete toxicity loss was obtained after the treatment using photocatalytic ozonation. The possible degradation pathway of the phthalate by oxidation was suggested based on aromatic ring opening reactions. The catalyst used at this experiment confirmed as a durable for continuous use

with almost no loss of activity over time. The design of the reactor was found to be very effective for water treatment using photocatalytic ozonation. Such design has a high potential and can be further upscaled to industrial applications due to the simplicity and versatility of manufacturing and maintenance.

**Keywords** Water pollution · Wastewater treatment · Advanced oxidation · Ozonation · Photocatalysis · Photocatalytic ozonation

## Introduction

Advanced oxidation (AO) technology undergoes an intensive scientific exploration for its ability to decompose persistent organic compounds in water, which are hardly degradable using conventional technologies (Tijani et al. 2014; Fernández-Castro et al. 2015). Generally, AO processes utilize the in situ formation of reactive hydroxyl and oxygen radicals which serve as oxidative agents. Such highly reactive environments are being achieved primarily by two techniques differing by reaction phases: homogeneous processes, based on the salvation of plasma ionized gas (including O<sub>3</sub>) or H<sub>2</sub>O<sub>2</sub> and Fe<sup>2+</sup> ions together with ultraviolet radiation (UV); or heterogeneous processes based on the application of a (photo)catalyst (Tijani et al. 2014). A combination of plasma/O<sub>3</sub> with UV/visible light photocatalysis was found to be very promising to increase the effectiveness of these processes as compared to the same methods used alone due to insufficient oxidation capability of ozone for some organic compounds (Martins and Quinta-Ferreira 2014; Mano et al. 2015; Huang et al. 2016; Moreira et al. 2016; Wei et al. 2017).

The oxidative species in non-thermal plasma reactors can be produced via in situ and ex situ processes. In in situ

Responsible editor: Vítor Pais Vilar

✉ Martynas Tichonovas  
martynas.tichonovas@ktu.lt

<sup>1</sup> Department of Environmental Technology, Kaunas University of Technology, Radvilenu pl. 19, LT-50254 Kaunas, Lithuania

systems, the discharge occurs on a gas/water contact surface, producing HO· radicals (Zhang et al. 2016a). In ex situ systems, active species are formed in gas, which is then delivered to water. The main product of ionization reactions in air is ozone, with trace amounts of nitrogen oxides (Simek et al. 2012; Pekárek and Mikeš 2014). Other reactive radicals, including HO·, have a very short life span (<0.5 s), thus are not being transferred from the reactor, but form in water as the product of the O<sub>3</sub> decomposition or UV radiation. Ex situ configuration is more feasible in upscaled reactors in a view of simplicity of design and a long-term maintenance.

Various photo and ozone heterogeneous catalysts were recently researched for their application for photocatalysis in plasma-based advanced oxidation wastewater treatment processes. Transition metal oxides or their mixtures, such as TiO<sub>2</sub>, MnO<sub>2</sub>, Fe<sub>2</sub>O<sub>3</sub>, WO<sub>3</sub> (Bloh et al. 2012; Mano et al. 2015; Xiao et al. 2015; Huang et al. 2016), elemental metal powders (Wen et al. 2014), or metal fibers (Zhu et al. 2014) were tested. UV-activated TiO<sub>2</sub> catalyst was proved as the most feasible catalyst for wastewater treatment, as the most stable and efficient (Mano et al. 2015; Xiao et al. 2015). Mostly, TiO<sub>2</sub> was introduced to wastewater in a powder form, making it difficult to remove after the treatment. TiO<sub>2</sub> immobilization on supports was used less frequently, usually utilizing micro-sized support particles (Choi et al. 2016), while experiments utilizing TiO<sub>2</sub> coatings on fixed support surfaces are rare. The use of immobilized heterogeneous catalyst for wastewater treatment has been suggested as technologically superior (Mehrojuei et al. 2015) due to avoided necessity of the separation of the catalyst from the treated water, such as in case of a powdered form of the catalyst.

Most of the reported data from the AO systems based on plasma-catalysis-UV simultaneous process has been reported from small laboratory-scale experiments, with reactor volumes up to 1 L, aiming to explore the reaction mechanisms, possible degradation products, and kinetics (Dai et al. 2014; Solís et al. 2016). There is lack of research devoted to the upscaling such AO systems to industrial level, which was emphasized in recent reviews (Nawrocki 2013; Xiao et al. 2015). Recent attempts to convert fundamental processes to technological upscaling include removal of contaminants of emerging concern (diclofenac, carbamazepine, etc.) from the water using photocatalytic ozonation reactor packed with TiO<sub>2</sub>-coated glass rings (Moreira et al. 2016), decomposition of emerging pollutants (antipyrine, bisphenol A, etc.) in municipal wastewater in solar photocatalytic reactor, working with powdered TiO<sub>2</sub> as catalyst (Quiñones et al. 2015), and degradation of methyl orange, amoxicillin and 3-chlorophenol using TiO<sub>2</sub>-coated silica gel beads in the photocatalysis reactor (Li et al. 2015).

The up to now data on the application of such AO setups for wastewater treatment indicated the following important

design parameters for an easily upscalable reactor construction:

- 1) Energy-efficient production of oxidative species. Nowadays, the dielectric barrier discharge (DBD) technique is the most efficient for the production of low temperature plasma containing ozone and other oxidative species (Wei et al. 2017). This may be achieved by the application of a high-voltage power converter working at the resonant mode with the reactor. Such principle is usually implemented in industrial ozonizers.
- 2) Energy efficient UV generation (Xiao et al. 2015). The most common source of UVC radiation is mercury luminescent lamps, which are comparatively energy efficient. The power of UV source must be calculated for the volume of treated water.
- 3) Catalyst configuration, activity, and durability. The catalyst must have high catalytic activity as well as to be inert and highly resistant to aging, to avoid wear and early replacement (Nawrocki 2013; Martins and Quinta-Ferreira 2014). While TiO<sub>2</sub> has been proved as the most suitable chemically, the configuration of the introduction of the catalyst, including proper support and layer quality, must be adequately solved in the upscaled reactors.
- 4) Optimal configuration of the running parameters (Tijani et al. 2014; Xiao et al. 2015). This technology is rather sensitive to the type of wastewater and the matrix that pollutants are dissolved in, including pH. This treatment method is applied for specific industrial wastewater containing relatively low concentrations of highly persistent organic pollutants. The optimum configuration between plasma, UV, and catalyst operation must be achieved, in addition to other engineering challenges for the prolongation of catalyst activity and highly efficient decomposition of pollutants.

In this study, we have addressed all of the above parameters, especially the catalyst configuration and the joint application of plasma-UV-catalysis system in the bench-scale AO-based wastewater treatment reactor. 2-naphthol, phenol, oxalic acid, phthalate, methylene blue, and D-glucose served as model pollutants, while the mixture of these compounds was used to simulate the real-life industrial wastewater. Full degradation of pollutants as determined by TOC value and a complete loss in toxicity was reached. We have proved that the AO method of plasma-UV-catalyst can be successfully applied for the treatment of wastewater containing hardly degradable organic compounds. The results provide background for the further investigations of this AO system to industrial applications, confirming the versatility of such reactor design and selected AO method.

## Materials and methods

### Experimental setup

The bench-scale advanced oxidation system based on plasma-UV-catalysis processes was designed and assembled at the Department of Environmental Technology at Kaunas University of Technology. The design of the DBD reactor for plasma production was similar as in our recent experiments in small-scale systems (Tichonovas et al. 2013; Krugly et al. 2015). The current setup was designed for bench-scale experiments for various combinations of plasma (ozonation) and photocatalysis processes to degrade pollutants in water. The principal scheme of the setup is presented in Fig. 1.

This setup is based on a batch operation, and employs a system of three vessels, each of 2 L volume. Initially, the wastewater is pumped to the buffer vessel (8) which has volume markers, to measure the amount needed for the experiments (1.6 L). Afterwards, the water is supplied either to the second vessel (9) (DBD plasma reactor vessel) or the third vessel (16) (photocatalysis reactor). The DBD plasma reactor (10) consists of a double wall quartz tube installed in the center of the vessel and containing a salt solution-based high-voltage central electrode and a gap between two quartz walls. The outer quartz wall surface is surrounded by the water when the device is under operation; the water in this vessel is electrically grounded and at the same time acts as a cooling medium for the reactor. The air is supplied to the gap of the DBD reactor, where the plasma forms when high-voltage

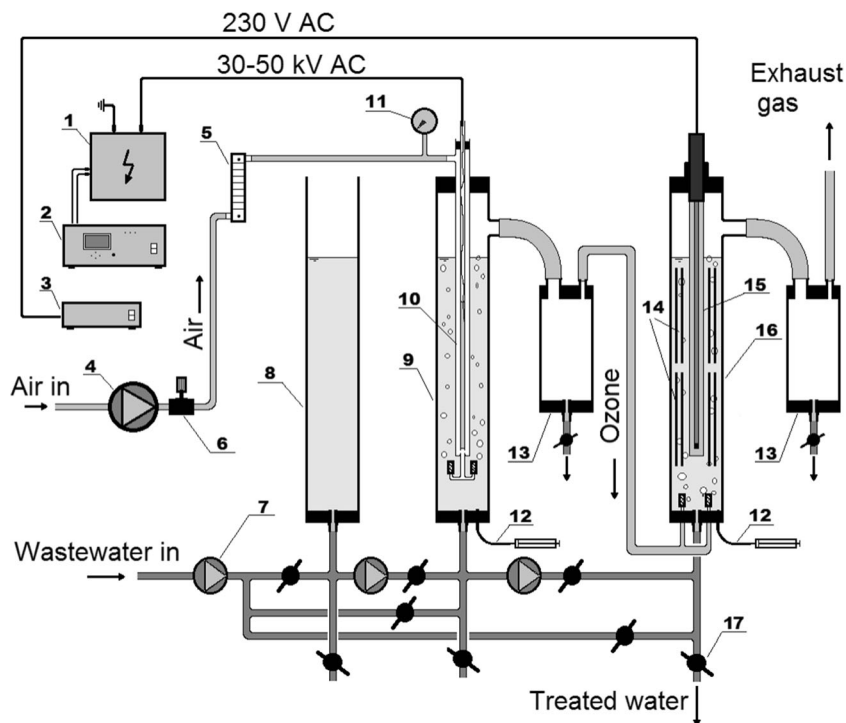
generation is activated. The formed plasma then is bubbled to the wastewater through ceramic diffusers in the same reactor. The third reactor has a UVC lamp (15) (40 W model F980078BU, LightTech, Hungary) installed in the middle of this vessel, and a frame for the mounting of catalyst (14), as well as the diffusers for bubbling remaining ozone from the DBD reactor. Thus, the third reactor employs all three factors—ozone, UV radiation, and catalyst.

In addition to reaction vessels, two foam dampers, air flow and UV controllers, power measurement unit, and the high-voltage generator are employed. The latter had a power control and the adjustment of frequency in the range of 1–10 kHz.

Such versatile system can be used to study the separate or simultaneous effects of plasma, UV and catalyst to the pollutant decomposition. In the further experiments, the DBD plasma reactor was used as an ozone generator, and all the decomposition processes with model wastewater were performed in the third vessel—UV reactor. For ozone generation purposes, the DBD reactor vessel was filled with clean synthetic tap water in each experiment; this water was changed before every run.

The ambient air was fed to the DBD reactor as the most feasible solution with almost zero costs. Such application is most likely to occur in industrial settings, although having less-efficient ozone generation compared to pure oxygen. The formation of nitrogen oxides occurs in air-based plasma, which can be partially responsible for pollutant degradation and may interfere with the pH of the treated water. The formation of  $\text{NO}_x$  has been shown to depend on the energy density of DBD reactor. Simek et al. (2012) has calculated  $\text{O}_3/$

**Fig. 1** Principal layout of the bench-scale advanced oxidation system for decomposition of wastewater pollutants: 1—high-voltage transformer, 2—high-voltage controller, 3—UV controller, 4—air supply pump, 5—rotameter, 6—air flow valve, 7—liquid pumps, 8—buffer vessel, 9—DBD reactor vessel, 10—DBD reactor, 11—pressure measurement, 12—sampling syringes, 13—foam damper, 14—frames of the catalyst, 15—UV lamp with quartz cover, 16—UV-photocatalysis reactor, 17—valves



NO<sub>x</sub> ratio equal to approx. 40 ± 8 at energy densities (10<sup>-3</sup>–10<sup>-2</sup> Wh/L) in air feed surface DBD reactor. Our setup has also operated at similar energy density values (4.3 × 10<sup>-2</sup> Wh/L at main experiment); thus, we refer to the mixture of ionized gas from the DBD reactor as ozone onwards.

### Catalyst preparation

The catalyst coating on glass was prepared using commercially available TiO<sub>2</sub> nanopowder Aeroxide P25, primary particle size 21 nm (Evonik Degussa GmbH, Germany). Glass rods (Simax) 5 mm in diameter and 20 cm in length were used as the catalyst support. The TiO<sub>2</sub> powder was dispersed into methanol at a concentration of 10 g/L and ultrasonicated for 30 min. The glass rods were positioned on a heating plate and sprayed with TiO<sub>2</sub>-methanol suspension using atomizer nozzle. The procedure was repeated several times to form uniform layer of the catalyst. The glass rods with TiO<sub>2</sub> coating were placed to the muffle furnace and heated at 450 °C for 3 h. The prepared rods were fastened in polytetrafluoroethylene (PTFE) and stainless steel frames. This frame consisted of two PTFE rings, which have been fastened in parallel position to each other with two stainless steel bolts. The rings had holes for mounting of glass rod ends. The 30 rods were positioned in a radial arrangement around the center of the cylindrical construction, with an orifice for UV lamp positioned in the center. Two frames of the prepared catalyst were installed in the reactor. The catalyst specific surface area in the reactor,

calculated as glass substrate surface area divided by wastewater volume was approximately 111.8 m<sup>2</sup>/m<sup>3</sup>.

### Model wastewater

Model wastewater was prepared using six compounds (Table 1)—2-naphthol, phenol, oxalic acid, potassium hydrogen phthalate, methylene blue, and D-glucose—representing pollutants in wastewater from various industrial processes. 2-naphthol, phenol, and phthalate were chosen due to their presence in wastewaters of chemical industries (Contreras et al. 2011). Methylene blue was selected as an example of a synthetic dye, which are common pollutants in textile industry wastewater (Tichonovas et al. 2013). Oxalic acid was widely used as a chemical resistant to ozonation (Orge et al. 2015). D-glucose was chosen as a potentially easy-to-degrade compound, which can compete with more persistent pollutants in oxidation reactions. All target chemicals and other chemicals were of an analytical grade. Synthetic tap water was prepared according to the methodology described by Morrow et al. (2008), using the distilled water (TOC value <0.1 mg/L, conductivity <15 µS/cm), and analytical grade inorganic reagents. Model wastewater was prepared by dissolving target organic compounds in the synthetic tap water according to concentrations presented in Table 1. In case of the mixture of the six compounds, the concentration of every compound was calculated according to the desired TOC value of 50 mg/L, i.e., equal to 8.33 mg/L of TOC for each compound. Such

**Table 1** Substances acting as pollutants in the model wastewater

Model wastewater no.	Substance name; CAS number	Concentration (mg/L)	Calculated TOC value (mg/L)	Measured TOC value (mg/L)	Measured initial pH value	Measured final pH value	Initial temperature (°C)	Final temperature (°C)
1	2-naphthol; 135-19-3	60.00	50.0	50.2	5.4	3.6–5.9	~18	~20 (without UV lamp operating) /~25 (with UV lamp operating)
2	Phenol; 108–95-2	65.35	50.0	51.6	5.4	3.7–5.7		
3	Oxalic acid (dihydrate); 144-62-7	262.64	50.0	51.4	2.7	3.2–4.3		
4	Potassium hydrogen phthalate; 877-24-7	106.36	50.0	50.3	4.3	3.5–4.3		
5	Methylene blue (trihydrate); 7220-79-3	97.36	50.0	43.1	5.4	3.7–5.2		
6	D-glucose (monohydrate); 50-99-7	137.61	50.0	52.1	5.7	3.6–5.3		
7	Mixture of all 6 pollutants	8.33 mg/L of TOC for each compound	50.0	50.1	3.4 3 7 11	3.3–4.0 3.3–3.8 5.9–6.2 8.2–8.7		

concentrations of specific pollutants may be on a higher range for a real industrial wastewater, but are suitable for the examination of decomposition technology. An efficient degradation at higher concentrations implies that the technology should be effective at lower concentrations as well. The prepared model wastewater was employed in experiments immediately after preparation, to avoid possible degradation and other reactions over time.

### The experimental design

**Optimal parameters of the DBD reactor and ozone production** The DBD reactor system was adjusted to the resonant frequency, with the aim to achieve the maximum power usage efficiency for conversion of low voltage to high voltage. This procedure is described in supplementary material.

**Efficiency of the AO system** This experiment aimed to determine the effects of various combinations of ozonation, UV, and catalysis to the pollutant decomposition. These experiments were carried out in the third (UV) reactor. The following combinations of parameters were set:

- Air (no ozone) + UV (photolysis)
- Air (no ozone) + UV + Catalyst (photocatalysis)
- O<sub>3</sub> only (ozonation)
- O<sub>3</sub> + UV (photolytic ozonation)
- O<sub>3</sub> + Catalyst (catalytic ozonation)
- O<sub>3</sub> + UV + Catalyst (photocatalytic ozonation)

The treatment efficacy was evaluated by measuring TOC of treated water. Of the model wastewater, 1.6 L was treated during every run.

All experiments lasted for 60 min, sampling in 10-min intervals (except oxalic acid, where additional samples at 5, 15, and 25 min were taken). Three repetitions of each test were made. The toxicity and UPLC-MS analyses were applied to photocatalytic ozonation experiments to identify the possible products of degradation and their toxicity.

**Influence of initial pH** The model wastewater no. 7 (mixture of all compounds) was used for testing the effects of the initial pH value to the decomposition efficiency for photocatalytic ozonation process. pH values of 3, 7, and 11 were tested, making adjustments with 0.1 M H<sub>2</sub>SO<sub>4</sub> or 0.1 M NaOH. The value of the pH was not controlled during the treatment.

**Determination of catalyst durability** The catalyst durability was measured by performing a series of photocatalytic ozonation experiments in a row using a fresh 2-naphthol model wastewater. Firstly, experiments with freshly prepared catalyst were conducted as a series of 10 experiments in a row. After approx. 100 h of operation of the same catalyst with various

pollutants, it was tested against 2-naphthol again, by measuring its activity during a series of 5 experiments. All durability experiments lasted for 30 min. SEM and XRD analyses were performed for characterization of new made and used catalyst, as well as the commercial powder sample.

### Analytical methods

**Power measurements** Power measurements of DBD reactor were made following a standard Lissajous power measurement method (Cai et al. 2010). The oscilloscope Rigol DS1052E (Rigol technologies, P.R.C.) and 1000× high-voltage probe (Tektronix, P.R.C.) was used for the measurements. A capacitor of  $6.8 \times 10^{-8}$  F was connected between DBD reactor and the ground during the measurements.

**Ozone production** Ozone concentration in gas phase was determined using a standard iodometric analysis method (Standardized Procedure 001/96).

**TOC analysis** TOC analyses were performed using TOC analyzer (TOC-L, Shimadzu, Japan) following the EN 1484:2002 standard.

**XRD and SEM analyses** The X-ray diffractometer D8 Advance (Bruker, USA) was used for XRD analysis, while SEM images were obtained by EVO MA 15 (Zeiss, Germany) electron microscope.

**UPLC-MS analysis** UPLC-MS analysis was performed using Acquity UPLC (Waters, USA) system equipped with a mass spectrometer Maixis 4G (Bruker, USA). The Acquity UPLC BEH C18 column was used for separation. 0.1% formic acid ( $v/v$ ) in ultrapure water and methanol were used as mobile phases. The MS was operated at the capillary voltage of 4500 V, nebulizer pressure of 2.5 bar and dry gas (nitrogen) flow of 10 L/min at the temperature of 200 °C. Ion polarity was set to negative, with scan range of 80–1200  $m/z$ .

**Toxicity testing** Toxicity of untreated and treated model wastewater samples were determined using adapted *Daphnia magna* toxicity testing procedure (Daphtoxkit F<sup>TM</sup>), (MicroBioTests Inc., Belgium). All samples were diluted two times before testing; three repetitions of each test were made. The daphnia mortality was checked after 24 h.

**Data analysis** The data were analyzed using Matlab7 software package. The linear and non-linear regression modeling was applied to estimate energy amounts required for pollutant degradation and to determine parameters of the decomposition kinetics.

## Results and discussion

### The parameters of the ozone generation in DBD reactor

A direct non-linear (logarithmic) relationship between the concentration of produced O<sub>3</sub> in air and the DBD power were observed (Fig. 2a) at all feed air flowrates. Such findings agree with results from other studies using DBD reactors (Mok et al. 2008; Pekárek and Mikeš 2014). The analysis of the ozone yield per consumed energy (Fig. 2b) suggested two points of optimal parameters, namely at 11 L/min of air flow and 28.8 W of DBD power (this combination was used for further experiments), as well as 15 L/min and 54.9 W, respectively.

### Characterization of the catalyst

The surface of the manufactured catalyst coating was relatively rough, as suggested by SEM imaging (Fig. 3a, b), with a uniform distribution of the TiO<sub>2</sub> layer and various protrusions in the size range between 1 and 10 μm. In fresh catalyst (Fig. 3a), some of these TiO<sub>2</sub> aggregates were as large as 5–10 μm, while they are not visible on a used catalyst surface (Fig. 3b), where only small sized (1–5 μm) aggregates of TiO<sub>2</sub> occur. The larger TiO<sub>2</sub> aggregates possibly were “fluffy” and loosely attached, and were washed away from the surface during the initial tests. Correspondingly, the degradation of 2-naphthol (which was run first) appeared as the most efficient. Such washout of the nanoparticle-based catalyst is unwanted in commercial applications due to the potentially adverse effects of released nanoparticles to aqueous ecosystems. Newly made catalysts must be pretreated by rinsing with distilled water before the installations in operational

environments, for washing possibly poorly attached TiO<sub>2</sub> particles after catalyst manufacturing process, to avoid the release of these particles to the treated water.

The crystalline structure of the new and used catalysts was the comparatively similar to each other and to the commercial powder (Fig. 3c). The ratio between the anatase and rutile phases in the coating remained the same as in commercial powder sample. Only the slight reduction of all peaks was observed, probably related to the agglomeration of nanopowder to larger particles during thermal processing.

After the first run, the activity of the catalyst decreased during succeeding runs, but remained stable (Fig. 4). The measured treatment efficiency was also comparatively stable (75%) during all series of durability testing experiments (1–10), except in the first two experiments where efficiencies were 78.9 and 76.9%. No significant loss of efficiency (72.9%) was observed after secondary durability testing (experiments 11–15). A low difference (2.4%) between new and used catalyst can have attributed to the mechanical wearing when installing and withdrawing catalyst constructions to the reactor between experiments and can be avoided in industrial installations assuming correct handling of catalyst frames.

In general, the construction of the catalyst coated glass rods surrounding the UV source proved to be efficient in upscaling to a bench scale, and potentially, to industrial scale.

### Degradation efficiency of pollutants by various combinations of AO components

The efficiency of the degradation of tested pollutants using various combinations of AO techniques are presented below, grouping to photolysis and photocatalysis, ozonation and

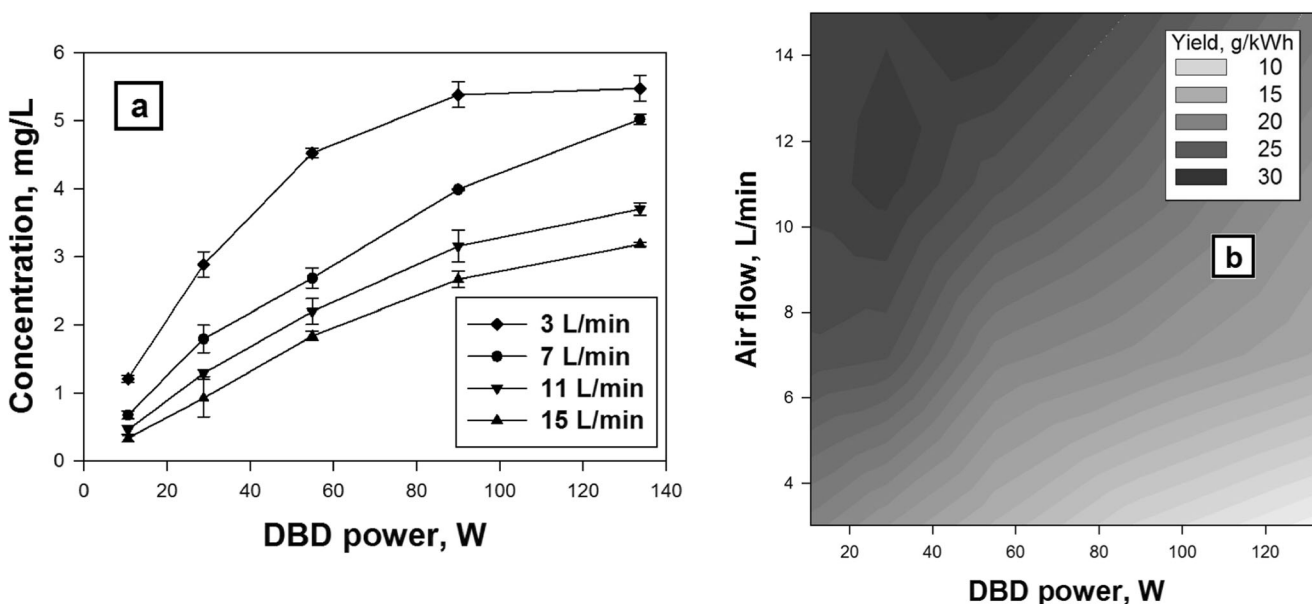


**Fig. 2** The generation of O<sub>3</sub> of the DBD reactor. **a** Ozone concentration (mg/L) obtained at various air flow rate (L/min) and DBD power (W) settings. **b** Ozone yield (g/kWh) at various air flow rate (L/min) and DBD power (W) settings

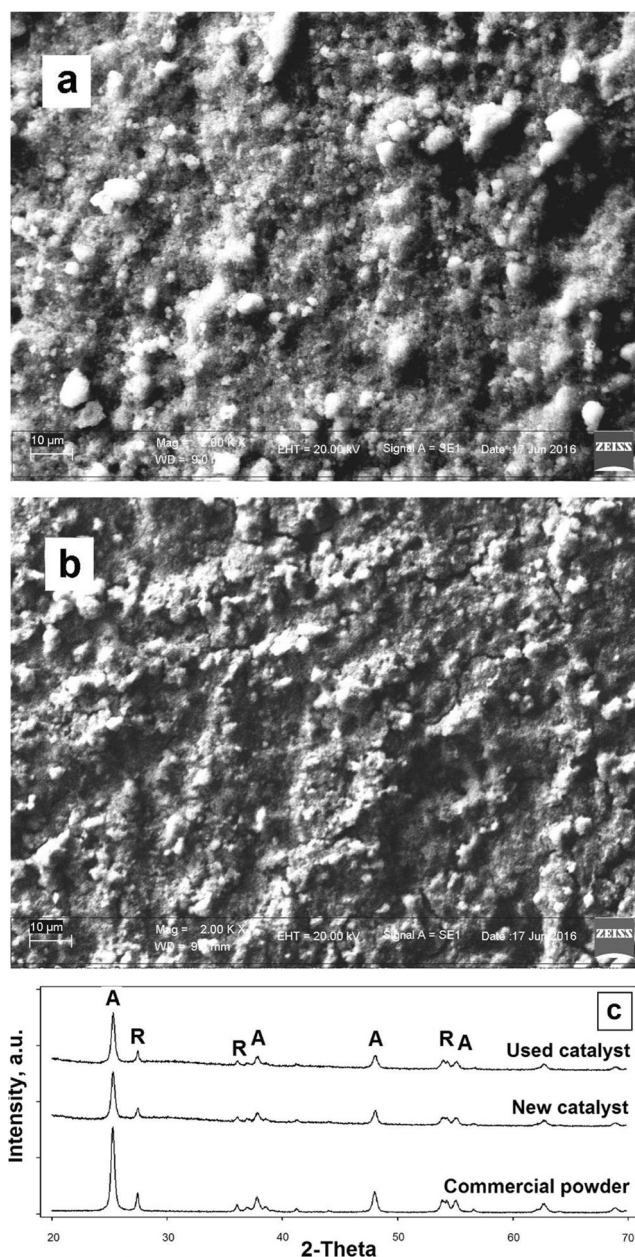


**Fig. 3** Catalyst characterization. **a** SEM image of a newly made catalyst. **b** SEM image of a used catalyst. **c** XRD spectrum of catalyst samples (R—rutile phase, A—anatase phase)

catalytic ozonation, as well as photolytic ozonation and photocatalytic ozonation. Such grouping was selected due to comparable performance of these techniques in the degradation process.

**Photolysis and photocatalysis** These two techniques performed the worst, with the slight increase in efficiency after the introduction of the catalyst. The decrease in TOC concentration during photolysis ranged from 0.4% in case of D-glucose to 99.7% in case of oxalic acid. During photocatalysis experiment, the TOC decrease ranged from 10.2 to 99.7%

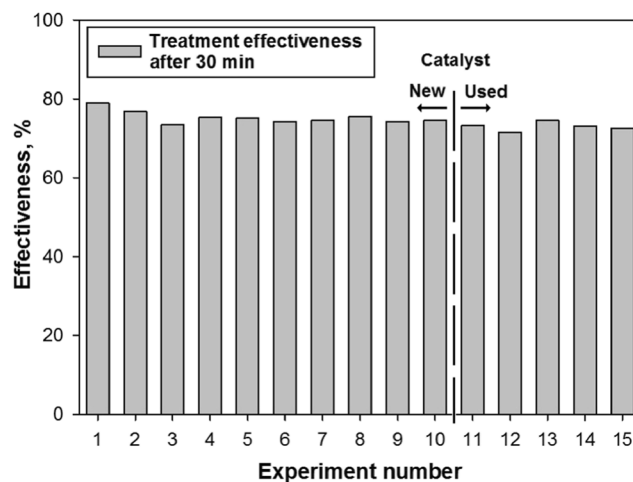


**Fig. 4** The change of decomposition efficiency vs catalyst aging. The first 10 experiments show the effectiveness of the photocatalytic ozonation using newly made catalyst; the last five show the same experiments with the used catalyst

using methylene blue and oxalic acid, respectively (Fig. 5a, b). Such poor performance indicates that the production of oxidative species was inefficient, except of oxalic acid. This has been noticed in earlier studies (Mano et al. 2015; Huang et al. 2016), suggesting the necessity of the introduction of ozone to initiate the more rapid decomposition process. At both photolysis and photocatalysis experiments, a strong foaming of model wastewater was observed during the first 10 min of 2-naphthol decomposition. The foam was carried off to the foam dampers with exhaust gas from the reactor. This lead to a notable reduction of TOC, because the organic matter was removed without degradation. After the foaming stopped, no significant TOC reduction was observed. This indicates that special measures must be taken to observe potential formation of foams in specific cases of industrial applications.

**Ozonation and catalytic ozonation** Ozonation and catalytic ozonation were slightly more efficient experimental conditions, providing the decrease in TOC values from 2.8% (oxalic acid) to 37.7% (phthalate) during ozonation and from 3.1% (D-glucose) to 48.9% (phthalate) during catalytic ozonation (Fig. 5c, d). Such small degradation efficiency was reported by other researchers, e.g., Orge et al. (2015) in case of oxalic acid. The obtained ranges of degradation are not suitable for industrial applications, where more rapid and complete degradation of pollutants is expected. Strong foam formation was registered this time during the degradation of methylene blue. The mechanisms behind the formation of foam have not been identified, but possibly related to the primary decomposition by-products or initial compound which can have foaming properties. It should be noted that the initial concentration of the pollutants was relatively high; thus, the foaming may be not so pronounced in industrial settings, although the presence

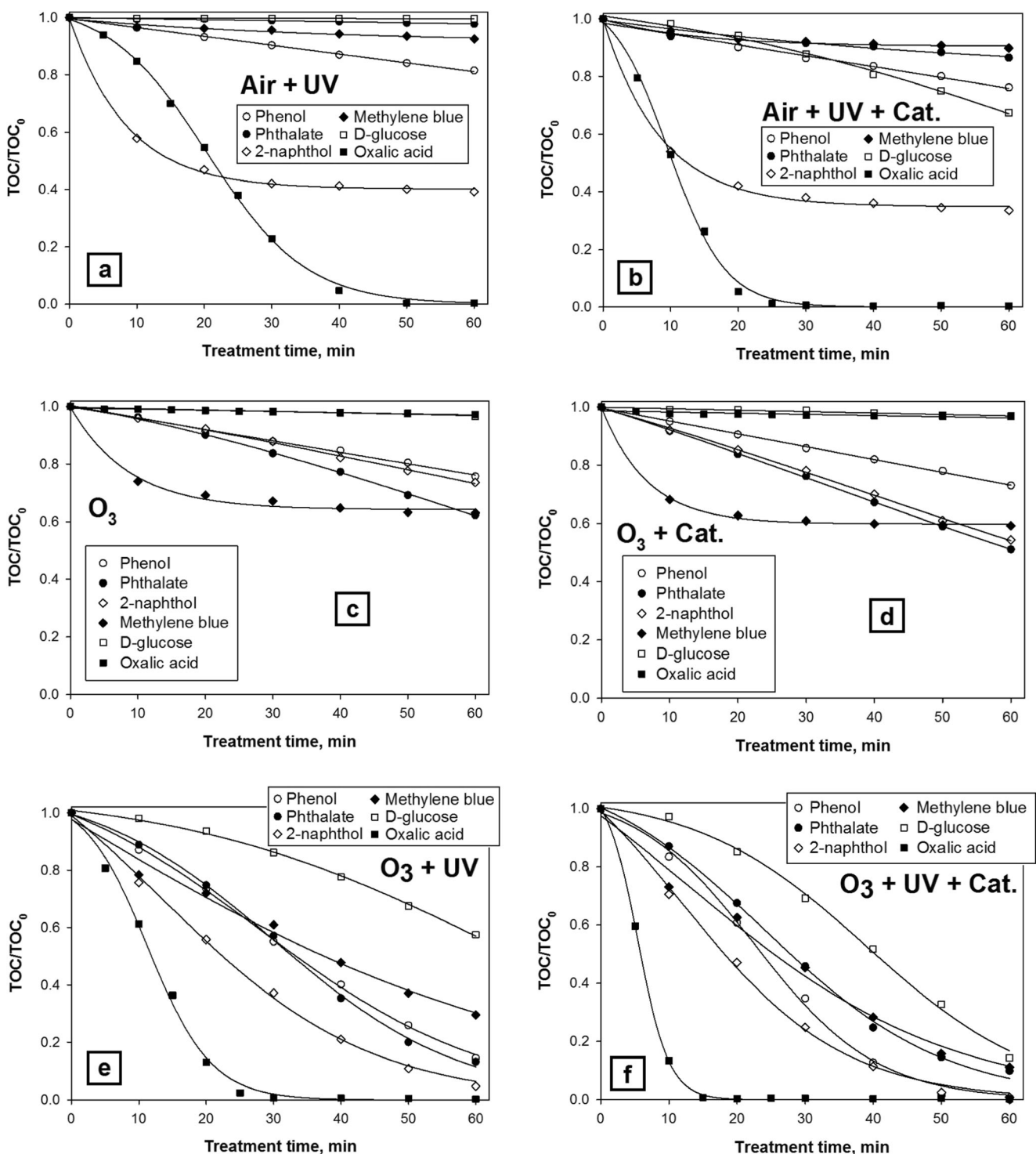


**Fig. 5** Decomposition kinetics and efficiency of tested compounds. Photolysis (a), photocatalysis (b), ozonation (c), catalytic ozonation (d), photolytic ozonation (e), and photocatalytic ozonation (f). The data is

given in relative units of measured TOC concentration. The linear and non-linear regression models are fitted at the graphs

of other matrix materials, such as surfactants, may be crucial for the operation of such technology. A slight increase of effectiveness during catalytic ozonation against purely ozonation may be explained by the mechanism, where the adsorbed ozone reacts with the TiO<sub>2</sub> surface (without UV

light) producing ozonide ions which later can be transformed to hydroxyl radicals (Hernández-Alonso et al. 2002).

**Photolytic ozonation and photocatalytic ozonation**  
Photolytic ozonation and photocatalytic ozonation



processes yielded the best decomposition efficiencies, achieving decomposition efficiency as high as 99.9% for phenol after 1 h of photocatalytic ozonation treatment (Fig. 5e, f). The similar results were found by Oh et al. (2006) (phthalate solution), where the photolytic ozonation showed much better results than just ozonation. Moreover, the foaming was comparatively less intense during these experiments.

The above data indicate that the photocatalytic ozonation ( $O_3+UV+Cat.$ ) was the most efficient process, capable in removing target compounds reaching 90–99% degradation after 1 h of treatment. While technically efficient, this combination should be further explored for its durability and robustness to be implemented in industrial settings.

**Degradation kinetics** The approximation of degradation kinetics by regression models allowed the estimation of time required for the 90% degradation efficiency, and the energy consumption for each target pollutant at every experimental condition (Table 2). The lowest energy requirement for the degradation was during photocatalytic ozonation and ranged between 0.16 and 2.16 MJ/g (oxalic acid and methylene blue, respectively). The photolytic ozonation was more energy demanding (0.34–3.58 MJ/g, oxalic acid and methylene blue, respectively). All other experimental conditions found to be much more energy demanding.

Three parameter exponential and sigmoidal decay functions observed to be most suitable to approximate the degradation kinetics during tested AO combinations. The exponential decay was appropriate to model the TOC concentration loss at experiments where foaming was observed, such as in 2-naphthol photolysis and photocatalysis, or methylene blue ozonation and catalytic ozonation. The foaming was rapid during the first minutes and then decreased, with practically no degradation during remaining treatment.

The three parameter sigmoidal models were found to be most representative for the modeling of the degradation kinetics where the TOC value was chosen as a main parameter for degradation measurements, as selected in this study. In cases where the kinetics is observed by the decrease of the concentration of the initial compound, the kinetics usually follows exponential decay (Oh et al. 2006; Li et al. 2015; Moreira et al. 2016), while sigmoid kinetics is rare (De Witte et al. 2010). We believe that the kinetics represented by the degradation of TOC is more meaningful as it shows the process of full mineralization of organic compound, representing full degradation and the overall efficiency of the process. The mechanism of TOC concentration variation is a result of the initial degradation of original compound to its by-products following step-by-step reactions (Marotta et al. 2011; Márquez et al. 2014; Dai et al. 2015; Tay and Madehi 2015; Krugly et al. 2015; Guo et al. 2016; Zhang et al. 2016b). During the first minutes of degradation, the reduction of organic carbon and production of  $CO_2$  is very low, as indicated by the upper asymptote of the

sigmoid curve. Such low rate of conversion to  $CO_2$  during the start of degradation was observed by Dobrin et al. (2013), where the corona discharge above water was used for the degradation of diclofenac. In the middle of the process, lower molecular mass compounds fully degrade to  $CO_2$  thus increasing the mineralization rate, represented by the steepest slope of the S-curve and the inflection point. The mineralization rate decreases when the residual organic carbon approaches 30%, represented by the lower asymptote.

The linear regression model was found to be suitable for negligible degradation results, as phenol, D-glucose or oxalic acid ozonation, where low or no degradation was achieved. In case of phenol degradation experiments, this model shows the possible reduction of phenol model wastewater TOC value due to loss by possible phenol evaporation, not degradation.

**System testing using mixed pollutants wastewater and various pH values** AO process has been shown to depend on the pH value of the wastewater (De Witte et al. 2010; Xiao et al. 2015), due to the changing reactions of ozone in water and production of active radicals. The mixture model wastewater (no. 7 in Table 1) containing a composition of hardly and easily degradable pollutants was tested against the pH of the solution in ozonation processes, measuring the effectiveness of the process as the portion of the remaining TOC concentration.

In case of uncontrolled initial pH (equal to 3.38), the photocatalytic ozonation provided the best degradation efficiency (97.8%, Fig. 6a). The photolytic ozonation reached 84.4%, while purely ozonation stayed at 18.2% after 60 min of treatment. Similar trends have been registered in the initial pH-adjusted experiments, where the photocatalytic ozonation performed best, and ozonation worst (Fig. 6b–d). However, the final efficiency varied broadly. The highest efficiency for photocatalytic ozonation of 96.6% occurred at pH = 3, which is comparable with unadjusted pH. Although the end result was almost similar, the kinetics of the pH = 3.38 degradation was slightly faster in the initial phases, while in case of pH = 3, the kinetics followed more of a sigmoidal pattern.

At the initial pH = 11, only 63.5% efficiency was measured using photocatalytic ozonation, for photolytic ozonation—57.5%, and 31.8% for ozonation. This implies that single ozonation, although least efficient overall, is more efficient using elevated pH values. Similar findings were obtained during the ozonation of ciprofloxacin (De Witte et al. 2010), phenol (Contreras et al. 2011), and textile dyes (Gomes et al. 2012). At high pH, the formation of  $HO\cdot$  radicals is facilitated by the reaction of  $O_3$  with hydroxyl ions (Mehrojuei et al. 2015):

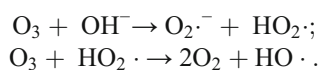


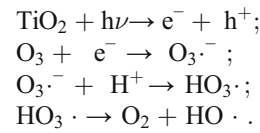
**Table 2** Regression models and calculated data, including the DBD energy and total energy (including UV lamp energy consumption) requirements for pollutant degradation, and time required to reach 90%

Model wastewater pollutant	Experimental conditions	Appropriate type of decay function	Degradation rate after 60 min of treatment (%)	Modeled time to decompose first 90% of TOC (min)	Modeled energy to decompose TOC (MJ)			Modeled energy to decompose 1 g of TOC until 90% treatment efficiency (MJ)			
					DBD	DBD + UV	DBD + UV	DBD	DBD + UV	DBD	DBD + UV
					0.43	0.43	0.43	5.96	5.96	4.96	4.96
2-naphthol	O <sub>3</sub>	Sigmoidal 3p.	26.4	248.3	0.43	0.43	0.43	5.96	5.96	4.96	4.96
	O <sub>3</sub> + Cat.	Sigmoidal 3p.	45.6	153.9	0.27	0.27	0.27	3.69	3.69	3.07	3.07
	O <sub>3</sub> + UV	Sigmoidal 3p.	95.2	52.8	0.09	0.22	0.22	1.27	3.03	1.05	2.52
	O <sub>3</sub> + UV + Cat.	Sigmoidal 3p.	99.2	41.7	0.07	0.17	0.17	1.00	2.39	0.83	1.99
	Air + UV	Exponential 3p.	66.5	>1000	0.00	>2.40	0.00	0.00	>33.33	0.00	>27.75
	Air + UV + Cat.	Exponential 3p.	60.8	>1000	0.00	>2.40	0.00	0.00	>33.33	0.00	>27.75
	O <sub>3</sub>	Linear	24.3	224.7	0.39	0.39	0.39	5.39	5.39	4.49	4.49
	O <sub>3</sub> + Cat.	Linear	27.0	203.5	0.35	0.35	0.35	4.89	4.89	4.07	4.07
Phenol	O <sub>3</sub> + UV	Sigmoidal 3p.	85.5	68.6	0.12	0.28	0.28	1.65	3.93	1.37	3.12
	O <sub>3</sub> + UV + Cat.	Sigmoidal 3p.	99.9	42.9	0.07	0.18	0.18	1.03	2.46	0.86	1.95
	Air + UV	Linear	23.8	288.9	0.00	0.69	0.69	0.00	9.63	0.00	7.37
	Air + UV + Cat.	Linear	18.5	232.9	0.00	0.56	0.56	0.00	7.76	0.00	5.94
	O <sub>3</sub>	Linear	2.8	>1000	>1.73	>1.73	>1.73	>24.00	>24.00	>6.40	>6.40
	O <sub>3</sub> + Cat.	Linear	3.3	>1000	>1.73	>1.73	>1.73	>24.00	>24.00	>6.40	>6.40
	O <sub>3</sub> + UV	Sigmoidal 3p.	99.7	22.0	0.04	0.09	0.09	0.53	1.26	0.14	0.34
	O <sub>3</sub> + UV + Cat.	Sigmoidal 3p.	99.7	10.7	0.02	0.04	0.04	0.26	0.61	0.07	0.16
Phthalate	Air + UV	Sigmoidal 3p.	99.7	37.0	0.00	0.09	0.09	0.00	1.23	0.00	0.33
	Air + UV + Cat.	Sigmoidal 3p.	99.7	19.3	0.00	0.05	0.05	0.00	0.64	0.00	0.17
	O <sub>3</sub>	Sigmoidal 3p.	37.7	155.6	0.27	0.27	0.27	3.73	3.73	1.76	1.76
	O <sub>3</sub> + Cat.	Sigmoidal 3p.	48.9	147.0	0.25	0.25	0.25	3.53	3.53	1.66	1.66
	O <sub>3</sub> + UV	Sigmoidal 3p.	86.8	62.2	0.11	0.26	0.26	1.49	3.56	0.70	1.68
	O <sub>3</sub> + UV + Cat.	Sigmoidal 3p.	90.2	55.4	0.10	0.23	0.23	1.33	3.18	0.62	1.49
	Air + UV	Linear	13.5	>1000	0.00	>2.40	0.00	0.00	>33.33	0.00	>15.67
	Air + UV + Cat.	Exponential 3p.	2.3	>1000	0.00	>2.40	0.00	0.00	>33.33	0.00	>15.67
Methylene blue	O <sub>3</sub>	Exponential 3p.	37.0	>1000	>1.73	>1.73	>1.73	>24.00	>24.00	>14.41	>14.41
	O <sub>3</sub> + Cat.	Exponential 3p.	40.7	>1000	>1.73	>1.73	>1.73	>24.00	>24.00	>14.41	>14.41
	O <sub>3</sub> + UV	Sigmoidal 3p.	70.5	104.1	0.18	0.43	0.43	2.50	5.97	1.50	3.58
	O <sub>3</sub> + UV + Cat.	Sigmoidal 3p.	88.8	62.8	0.11	0.26	0.26	1.51	3.60	0.91	2.16
	Air + UV	Exponential 3p.	10.2	>1000	0.00	>2.40	0.00	0.00	>33.33	0.00	>20.01
	Air + UV + Cat.	Exponential 3p.	7.5	>1000	0.00	>2.40	0.00	0.00	>33.33	0.00	>20.01
	O <sub>3</sub>	Linear	3.5	>1000	>1.73	>1.73	>1.73	>24.00	>24.00	>9.59	>9.59
	D-glucose	Linear	3.5	>1000	>1.73	>1.73	>1.73	>24.00	>24.00	>9.59	>9.59

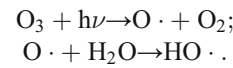
Table 2 (continued)

Model wastewater pollutant	Experimental conditions	Appropriate type of decay function	Degradation rate after 60 min of treatment (%)	Modeled time to decompose first 90% of TOC (min)	Modeled energy to decompose TOC (MJ)			Modeled energy to decompose 1 g of TOC until 90% treatment efficiency (MJ)			Modeled energy to decompose 1 g of pollutant until 90% treatment efficiency (MJ)		
					DBD		DBD + UV	DBD		DBD + UV	DBD		DBD + UV
					>1.73	>1.73	>1.73	>24.00	>24.00	>24.00	>24.00	>11.33	>11.33
Mixture	O <sub>3</sub> + Cat.	Linear	3.1	>1000	>1.73	>1.73	>24.00	>9.59	>24.00	>9.59	>24.00	>9.59	
	O <sub>3</sub> + UV	Sigmoidal 3p.	42.5	116.5	0.20	0.48	2.80	1.12	6.68	1.12	6.68	2.67	
	O <sub>3</sub> + UV + Cat.	Sigmoidal 3p.	85.6	67.4	0.12	0.28	1.62	0.65	3.86	0.65	3.86	1.54	
	Air + UV	Linear	32.6	>1000	0.00	>2.40	0.00	0.00	>33.33	0.00	>33.33	>13.32	
	Air + UV + Cat.	Sigmoidal 3p.	0.4	151.4	0.00	0.36	0.00	0.00	5.05	0.00	5.05	2.02	
	O <sub>3</sub>	Exponential 3p.	18.2	>1000	>1.73	>1.73	>24.00	>11.33	>24.00	>11.33	>24.00	>11.33	
	O <sub>3</sub> + Cat.	Exponential 3p.	18.0	>1000	>1.73	>1.73	>24.00	>11.33	>24.00	>11.33	>24.00	>11.33	
	O <sub>3</sub> + UV	Sigmoidal 3p.	84.4	69.1	0.12	0.29	1.66	0.78	3.96	0.78	3.96	1.87	
	O <sub>3</sub> + UV + Cat.	Sigmoidal 3p.	97.8	42.2	0.07	0.17	1.01	0.48	2.42	0.48	2.42	1.14	
	Air + UV	Exponential 3p.	39.7	>1000	0.00	>2.40	0.00	0.00	>33.33	0.00	>33.33	>15.74	
Air + UV + Cat.	Exponential 3p.	25.9	>1000	0.00	>2.40	0.00	0.00	>33.33	0.00	>33.33	>15.74		

On the other hand, the photocatalytic ozonation using TiO<sub>2</sub> as catalyst is more efficient at low pH values (Sánchez et al. 1998; Gimeno et al. 2007). Formation of ozonide (O<sub>3</sub><sup>-</sup>) radical under photocatalytic ozonation conditions and subsequent reaction chain with H<sup>+</sup> ion to form HO· radicals has been suggested as a prevailing mechanism (Sánchez et al. 1998; Mehrjouei et al. 2015):



The UV effect on ozone utilization is explained as a radiation induced oxygen radical formation and further water decomposition to HO· radicals (Mehrjouei et al. 2015):



The selection of AO technology in upscaled systems thus may depend on the pH of the wastewater. In cases of high pH, it may be more profitable to use ozonation with longer treatment duration, or to adjust pH before the treatment. The use of photocatalytic ozonation should be applied to wastewaters of low pH.

The reduction of the pH was registered in most cases (Table 1). This is associated with the fact that the formed degradation by-products often contain low-molecular weight organic acids (Marotta et al. 2011). The decrease of pH is also associated with the efficiency of the degradation process. In case of full mineralization (95–100% TOC reduction), the pH has remained similar to initial solution (when the initial compound was non-acidic) or increased (in case of oxalic acid). In less efficient processes, with total TOC reduction of ~40–80%, the pH tend to decrease due to increasing concentration of organic acids as by-products. In low efficiency processes, with total TOC reduction of ~10–40%, the pH remained at similar levels to initial solution due to minimal degradation of initial substance.

### Identification of decomposition by-products

Three samples of wastewater containing phthalate as the most persistent compound (excluding D-glucose as a non-hazardous substance) were analyzed, including the untreated sample with 100% initial TOC concentration, half-treated sample with 50% TOC concentration, and sample after 60 min of treatment. The time needed to treat the model wastewater to remaining 50% TOC value (27 min) was calculated from experiment on catalyst activity testing. Various phthalate degradation products were found in half-treated wastewater sample, including salicylic, 4-hydroxyphthalic, adipic acids,

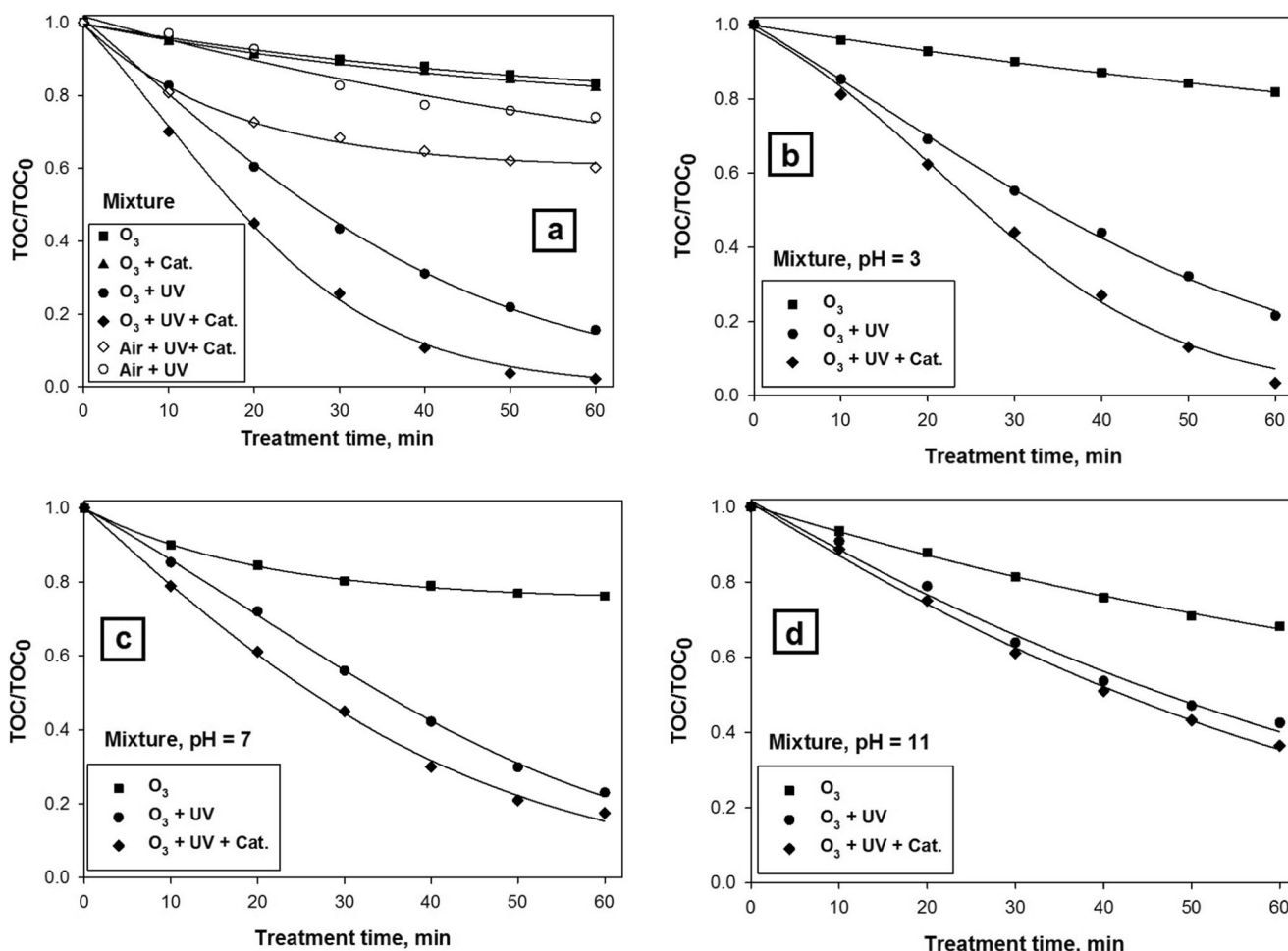


**Fig. 6** The effect of pH on the degradation efficiency of mixture wastewater as represented by TOC decrease. **a** Uncontrolled initial pH, **b** Artificially adjusted initial pH = 3, **c** pH = 7, and **d** pH = 11

and salicylaldehyde. The proposed simplified pathway is presented in Fig. 7. Possibly, the phthalate firstly degraded to salicylic acid and salicylaldehyde and then to adipic acid while losing the aromaticity. Formation of various acids, including aromatic ring containing and linear dicarboxylic acids, was observed by Q. Zhang et al. (2016b) where

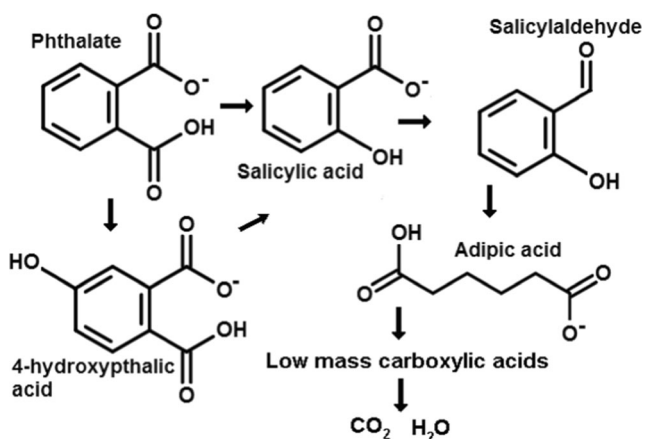


**Fig. 7** Formation of phthalate degradation by-products

Fenton oxidation was used for the phthalate degradation. The 4-hydroxyphthalic acid was formed from phthalate with accession of HO· radical directly to the aromatic ring. The direct accession of HO· radical to aromatic ring structure to form various hydroxybenzoates was also confirmed by Yuan et al. 2008 and Q. Zhang et al. 2016b. It should be noted that many more by-products are forming during the degradation of phthalate, but they are not detected due to low concentrations. No significant peaks were observed in the mass spectrum after 60 min of degradation, suggesting that the residual carbon (as measured with TOC analyzer) consisted of a wide range of organic compounds of a high state of the oxidation, such as simple organic acids. These compounds are comparatively less toxic and can be degraded completely to CO<sub>2</sub> and water with extended treatment time.

**Toxicity of decomposition by-products**

The toxicity of the model wastewater corresponds to the toxicity of the dissolved pollutant. The oxalic acid, methylene blue, 2-naphthol, and the mixture of all model pollutants were

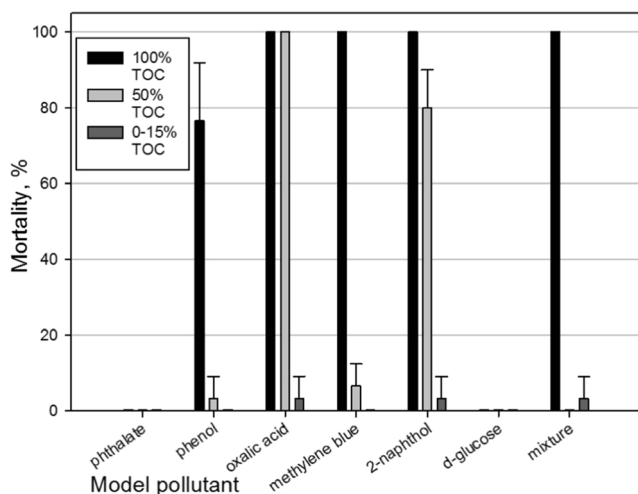


**Fig. 8** The mortality of *Daphnia magna* after 24 h, three samples of each model wastewater were examined—untreated, half treated (by TOC value), and after 1 h of treatment using photocatalytic ozonation

identified as very toxic (100% mortality) at applied concentrations (Fig. 8). The phenol solution was observed as least toxic (~80% mortality). The phthalate and D-glucose at selected concentrations were identified as non-toxic in all cases and in all treated wastewater samples.

Phenol, methylene blue and the mixture solutions have lost their toxicity after 50% TOC removal. The toxicity of the 2-naphthol solution was reduced by 20%, while oxalic acid remained as toxic as the initial solution. Our results suggest that the photocatalytic ozonation has a potential to fully reduce the toxicity of various toxic substances and their mixtures present in industrial wastewater. The treatment to the residual TOC of 0–15% is sufficient to reduce the toxicity to almost zero.

## Conclusions

The photocatalytic ozonation ( $O_3+UV+TiO_2$  catalyst) was successfully applied in a bench-scale advanced oxidation system. The efficiency of this technology for the degradation of various organic compounds in a model wastewater was proved based on the following parameters:

- The degradation efficiency reached 85.6–99.9% based on the TOC reduction after 60 min of treatment.
- The energy requirements are low (0.16 to 2.16 MJ/g of pollutant), including the energy for the production of ozone and generation of UV, as compared against other combinations of ozone/UV/catalysis.
- Complete loss in toxicity of wastewater has been reached after 60 min of treatment, resulted by the decomposition of persistent compounds (such as phthalate) to low-molecular weight acids and  $CO_2$ .

- The technology performed well in the wide range (3–11) of initial pH of a wastewater.
- The stationary  $TiO_2$ -coated glass catalyst has proved as durable and effective for the ozone-based AO wastewater treatment technology, assuming that the nanoparticles are well adhered to the mounting substrate.

The presented design of the photocatalytic ozonation reactor has a high potential to be upscaled to the industrial AO system.

**Acknowledgements** This work was supported by Research Council of Lithuania under grant “Synergetic effects in DBD (Dielectrical Barrier Discharge) plasma technology for removal of organic compounds from wastewater” (Sinergoplas), project no. MIP-024/2014.

## References

- Bloh JZ, Dillert R, Bahnemann DW (2012) Transition metal-modified zinc oxides for UV and visible light photocatalysis. *Environ Sci Pollut Res* 19:3688–3695. doi:10.1007/s11356-012-0932-y
- Cai YX, Zhang LF, Wang J, et al (2010) RETRACTED ARTICLE: measuring DBD main discharge parameters using Q-V Lissajous figures. *Asia-Pacific Power Energy Eng Conf APPEEC* 1–4. doi: 10.1109/APPEEC.2010.5449431
- Choi YI, Jeon KH, Kim HS et al (2016)  $TiO_2/BiOX$  (X = Cl, Br, I) hybrid microspheres for artificial waste water and real sample treatment under visible light irradiation. *Sep Purif Technol* 160:28–42. doi: 10.1016/j.seppur.2016.01.009
- Contreras EM, Bertola NC, Zaritzky NE (2011) Monitoring the ozonation of phenol solutions at constant pH by different methods. *Ind Eng Chem Res* 50:9799–9809. doi:10.1021/ie200999h
- Dai Q, Wang J, Yu J et al (2014) Catalytic ozonation for the degradation of acetylsalicylic acid in aqueous solution by magnetic  $CeO_2$  nanometer catalyst particles. *Appl Catal B Environ* 144:686–693. doi:10.1016/j.apcatb.2013.05.072
- Dai Q, Chen L, Chen W, Chen J (2015) Degradation and kinetics of phenoxyacetic acid in aqueous solution by ozonation. *Sep Purif Technol* 142:287–292. doi:10.1016/j.seppur.2014.12.045
- De Witte B, Van Langenhove H, Demeestere K et al (2010) Ciprofloxacin ozonation in hospital wastewater treatment plant effluent: effect of pH and  $H_2O_2$ . *Chemosphere* 78:1142–1147. doi:10.1016/j.chemosphere.2009.12.026
- Dobrin D, Bradu C, Magureanu M et al (2013) Degradation of diclofenac in water using a pulsed corona discharge. *Chem Eng J* 234:389–396. doi:10.1016/j.cej.2013.08.114
- Fernández-Castro P, Vallejo M, San Román MF, Ortiz I (2015) Insight on the fundamentals of advanced oxidation processes: role and review of the determination methods of reactive oxygen species. *J Chem Technol Biotechnol* 90:796–820. doi:10.1002/jctb.4634
- Gimeno O, Rivas FJ, Beltrán FJ, Carbajo M (2007) Photocatalytic ozonation of winery wastewaters. *J Agric Food Chem* 55:9944–9950. doi:10.1021/jf072167i
- Gomes AC, Fernandes LR, Simões RMS (2012) Oxidation rates of two textile dyes by ozone: effect of pH and competitive kinetics. *Chem Eng J* 189–190:175–181. doi:10.1016/j.cej.2012.02.051
- Guo Y, Lin Q, Xu B, Qi F (2016) Degradation of benzophenone-3 by the ozonation in aqueous solution: kinetics, intermediates and toxicity. *Environ Sci Pollut Res* 23:7962–7974. doi:10.1007/s11356-015-5941-1

- Hernández-Alonso D, Coronado JM, Maira AJ et al (2002) Ozone enhanced activity of aqueous titanium dioxide suspensions for photocatalytic oxidation of free cyanide ions. *Appl Catal B Environ* 39: 257–267
- Huang J, Wang X, Pan Z et al (2016) Efficient degradation of perfluorooctanoic acid (PFOA) by photocatalytic ozonation. *Chem Eng J* 296:329–334. doi:10.1016/j.cej.2016.03.116
- Krugly E, Martuzevicius D, Tichonovas M et al (2015) Decomposition of 2-naphthol in water using a non-thermal plasma reactor. *Chem Eng J* 260:188–198
- Li D, Zhu Q, Han C et al (2015) Photocatalytic degradation of recalcitrant organic pollutants in water using a novel cylindrical multi-column photoreactor packed with TiO<sub>2</sub>-coated silica gel beads. *J Hazard Mater* 285:398–408. doi:10.1016/j.jhazmat.2014.12.024
- Mano T, Nishimoto S, Kameshima Y, Miyake M (2015) Water treatment efficacy of various metal oxide semiconductors for photocatalytic ozonation under UV and visible light irradiation. *Chem Eng J* 264: 221–229. doi:10.1016/j.cej.2014.11.088
- Marotta E, Schiorlin M, Ren X et al (2011) Advanced oxidation process for degradation of aqueous phenol in a dielectric barrier discharge reactor. *Plasma Process Polym* 8:867–875. doi:10.1002/ppap.201100036
- Márquez G, Rodríguez EM, Maldonado MI, Álvarez PM (2014) Integration of ozone and solar TiO<sub>2</sub>-photocatalytic oxidation for the degradation of selected pharmaceutical compounds in water and wastewater. *Sep Purif Technol* 136:18–26. doi:10.1016/j.seppur.2014.08.024
- Martins RC, Quinta-Ferreira RM (2014) A review on the applications of ozonation for the treatment of real agro-industrial wastewaters. *Ozone Sci Eng* 36:3–35. doi:10.1080/01919512.2013.842158
- Mehrijouei M, Müller S, Möller D (2015) A review on photocatalytic ozonation used for the treatment of water and wastewater. *Chem Eng J* 263:209–219. doi:10.1016/j.cej.2014.10.112
- Mok YS, Jo J-O, Whitehead JC (2008) Degradation of an azo dye Orange II using a gas phase dielectric barrier discharge reactor submerged in water. *Chem Eng J* 142:56–64. doi:10.1016/j.cej.2007.11.012
- Moreira NFF, Sousa JM, Macedo G et al (2016) Photocatalytic ozonation of urban wastewater and surface water using immobilized TiO<sub>2</sub> with LEDs: micropollutants, antibiotic resistance genes and estrogenic activity. *Water Res* 94:10–22. doi:10.1016/j.watres.2016.02.003
- Morrow JB, Almeida JL, Fitzgerald LA, Cole KD (2008) Association and decontamination of *Bacillus* spores in a simulated drinking water system. *Water Res* 42:5011–5021. doi:10.1016/j.watres.2008.09.012
- Nawrocki J (2013) Catalytic ozonation in water: controversies and questions. Discussion paper. *Appl Catal B Environ* 142–143:465–471. doi:10.1016/j.apcatb.2013.05.061
- Oh BS, Jung YJ, Oh YJ et al (2006) Application of ozone, UV and ozone/UV processes to reduce diethyl phthalate and its estrogenic activity. *Sci Total Environ* 367:681–693. doi:10.1016/j.scitotenv.2006.02.051
- Orge CA, Pereira MFR, Faria JL (2015) Photocatalytic ozonation of model aqueous solutions of oxalic and oxamic acids. *Appl Catal B Environ* 174–175:113–119. doi:10.1016/j.apcatb.2015.02.038
- Pekárek S, Mikeš J (2014) Temperature- and airflow-related effects of ozone production by surface dielectric barrier discharge in air. *Eur Phys J D* 68:310. doi:10.1140/epjd/e2014-50393-x
- Quiñones DH, Álvarez PM, Rey A, Beltrán FJ (2015) Removal of emerging contaminants from municipal WWTP secondary effluents by solar photocatalytic ozonation. A pilot-scale study. *Sep Purif Technol* 149:132–139. doi:10.1016/j.seppur.2015.05.033
- Sánchez L, Peral J, Domènech X (1998) Aniline degradation by combined photocatalysis and ozonation. *Appl Catal B Environ* 19:59–65. doi:10.1016/S0926-3373(98)00058-7
- Simek M, Pekárek S, Prukner V (2012) Ozone production using a power modulated surface dielectric barrier discharge in dry synthetic air. *Plasma Chem Plasma Process* 32:743–754. doi:10.1007/s11090-012-9382-z
- Solís RR, Rivas FJ, Martínez-Piernas A, Agüera A (2016) Ozonation, photocatalysis and photocatalytic ozonation of diuron: intermediates identification. *Chem Eng J* 292:72–81. doi:10.1016/j.cej.2016.02.005
- Tay KS, Madehi N (2015) Ozonation of ofloxacin in water: by-products, degradation pathway and ecotoxicity assessment. *Sci Total Environ* 520:23–31. doi:10.1016/j.scitotenv.2015.03.033
- Tichonovas M, Krugly E, Racys V et al (2013) Degradation of various textile dyes as wastewater pollutants under dielectric barrier discharge plasma treatment. *Chem Eng J* 229:9–19
- Tijani JO, Fatoba OO, Madzivire G, Petrik LF (2014) A review of combined advanced oxidation technologies for the removal of organic pollutants from water. *Water Air Soil Pollut*. doi:10.1007/s11270-014-2102-y
- Wei C, Zhang F, Hu Y et al (2017) Ozonation in water treatment: the generation, basic properties of ozone and its practical application. *Rev Chem Eng* 33:49–89. doi:10.1515/revce-2016-0008
- Wen G, Wang SJ, Ma J et al (2014) Enhanced ozonation degradation of di-n-butyl phthalate by zero-valent zinc in aqueous solution: performance and mechanism. *J Hazard Mater* 265:69–78. doi:10.1016/j.jhazmat.2013.11.038
- Xiao J, Xie Y, Cao H (2015) Organic pollutants removal in wastewater by heterogeneous photocatalytic ozonation. *Chemosphere* 121:1–17. doi:10.1016/j.chemosphere.2014.10.072
- Yuan B-L, Li X, Graham N (2008) Rate-limited mass transfer of octane, decane, and dodecane into nonionic surfactants solutions under laminar flow conditions. *Chemosphere* 72:197–204. doi:10.1016/j.chemosphere.2008.01.055
- Zhang C, Fang Z, Liu W et al (2016a) Rapid removal of bacterial endotoxin and natural organic matter in water by dielectric barrier discharge plasma: efficiency and toxicity assessment. *J Hazard Mater* 318:15–23. doi:10.1016/j.jhazmat.2016.06.036
- Zhang Q, Wang C, Lei Y (2016b) Fenton's oxidation kinetics, pathway, and toxicity evaluation of diethyl phthalate in aqueous solution. *J Adv Oxid Technol* 19:125–133
- Zhu SN, Hui KN, Hong X, Hui KS (2014) Catalytic ozonation of basic yellow 87 with a reusable catalyst chip. *Chem Eng J* 242:180–186. doi:10.1016/j.cej.2013.12.041